Network Pharmacology and Experimental Validation of the Anti-tumor Mechanisms of Ginsenoside Rh2

Long ZHANG[1Δ], Shuangsen LIU[1Δ], Qin HUANG[1], Yue ZHOU[1], Feng XIONG[1], Nongyi LI[2], Yanni ZHANG[1*], Jue LIU[1*], Xinglong HUANG[1*]

1. Hospital of Traditional Chinese Medicine in Qijiang District, Chongqing Municipality, Chongqing 401420, China; 2. Chongqing College of Traditional Chinese Medicine, Chongqing 402760, China

Abstract [**Objectives**] To elucidate the mechanisms by which ginsenoside Rh2 inhibits the proliferation of breast cancer cells. [**Methods**] The effects of ginsenoside Rh2 on bone marrow-derived dendritic cells (BMDCs) in breast cancer-bearing mice were assessed using network pharmacology analysis, cytological assays, and protein histology techniques. The regulatory mechanisms of ginsenoside Rh2 on BMDCs were further explored via flow cytometry, enzyme-linked immunosorbent assay (ELISA), Western blot (WB), and reverse transcription polymerase chain reaction (RT-PCR). [**Results**] Network pharmacology analysis identified ginsenoside Rh2 as a potential therapeutic agent that facilitates dendritic cell (DC) maturation, with phosphoinositide 3-kinase regulatory subunit 1 (PIK3R1) serving as a crucial mediator. Experimental results confirmed that ginsenoside Rh2 enhanced BMDC maturation in breast cancer models via the PIK3R1-PDK1 signaling pathway. This enhancement coincided with decreased mRNA and protein expression levels of PIK3R1 and PDK1 in mouse DCs. [**Conclusions**] This study elucidates the potential molecular mechanisms of ginsenoside Rh2 through network pharmacology, which are subsequently validated by comprehensive laboratory experiments. Our findings indicate that ginsenoside Rh2 enhances tumor immunity and exerts anti-tumor effects by promoting DC maturation. Compared to conventional chemotherapy, ginsenoside Rh2 significantly reduces off-target toxicity while improving anti-tumor efficacy. In summary, this research provides novel insights and a theoretical foundation for the selection and development of breast cancer treatment regimens.

Key words Ginsenoside, Tumor immunology, PIK3R1-PDK1 signaling pathway, Dendritic cells, Breast cancer

1 Introduction

Over the past two decades, significant progress has been achieved in the treatment of breast cancer. Therapeutic strategies have evolved from radical mastectomy to breast-conserving surgery (BCS) and personalized therapies[1-2]. Advances in surgical techniques have facilitated the widespread adoption of BCS as an alternative to radical mastectomy, thereby minimizing physical trauma and improving postoperative quality of life[3-4]. Furthermore, advancements in early detection and personalized therapies have significantly increased patient survival rates[5-6].

Therapeutically, endocrine therapy and immunotherapy have provided additional options for breast cancer patients. Endocrine agents, such as tamoxifen and letrozole, have been demonstrated to effectively reduce the risk of breast cancer recurrence[7-9]. Advances in immunotherapy have also introduced novel therapeutic strategies. Antibody-drug conjugates (ADCs), including sacituzumab govitecan-hziy, have been shown to significantly improve patient survival outcomes[10-12]. These therapeutic advances have contributed not only to enhanced survival rates, but also to improvements in patients' quality of life.

However, several challenges remain in the treatment of breast cancer. First, the heterogeneity and invasiveness of certain breast cancer subtypes present major clinical obstacles. Although chemotherapy is a primary treatment modality, its long-term prognostic benefits need further enhancement[13]. In addition, treatment strategies continue to evolve, with risk-tailored therapies emerging to minimize unnecessary toxicity[14].

Ginsenosides, the primary bioactive components of ginseng, exhibit extensive pharmacological properties, including immune enhancement and anti-tumor activities[15-16]. However, research on the effects of ginsenosides on DCs in breast cancer remains limited, and the underlying mechanisms are inadequately understood. Previous studies involving bone marrow-derived dendritic cells (BMDCs) from breast cancer-bearing mice have demonstrated that ginsenosides significantly enhance immune responses. Specifically, ginsenosides markedly increased BMDC maturation, migratory capacity, and stimulated T and B lymphocyte proliferation. Based on prior research, ginsenosides Rh1, Rh2, Rh3, Rg3, and Rg5, known for anti-tumor properties, were evaluated for their impact on DC maturation in tumor-bearing mice[17-19]. Among these, Rh2 exhibited the strongest effect on DC maturation and function[20-22]. Hence, this study focused on ginsenoside Rh2, aiming to provide novel insights for the development of therapeutic agents against breast cancer.

2 Materials and methods

2.1 Data sources and study methods

2.1.1 Chemical structure and target identification of ginsenoside

Received: August 8, 2026 Accepted: September 15, 2026
Supported by Natural Science Foundation of Chongqing, China (CSTB2022NSCQ-MSX1569).

Δ These authors contributed equally to this work.
Long ZHANG, master's degree, associate chief physician; Shuangsen LIU, master's degree, associate chief physician. * Corresponding author. Yanni ZHANG, bachelor's degree, attending traditional Chinese medicine physician; Jue LIU, bachelor's degree, associate chief pharmacist; Xinglong HUANG, master's degree, pharmacist-in-charge.

Rh2. In March 2025, the SwissTargetPrediction platform (http://www.swisstargetprediction.ch/) and the SuperPred tool (https://prediction.charite.de/) were initially used to identify potential targets of ginsenoside Rh2. The resulting targets were cross-referenced with the UniProt database (https://www.uniprot.org/) to ensure accurate classification and verification. Non-human genes were eliminated, redundant entries were removed, and gene names were standardized.

2.1.2 Acquisition of DC maturation-related targets mediated by ginsenoside Rh2. The intersection between potential Rh2 targets predicted by SwissTargetPrediction and genes highly expressed in immature DCs from the GSE15076 dataset was analyzed. This analysis identified 20 genes as potential targets involved in Rh2-mediated DC maturation.

2.1.3 Protein-protein interaction (PPI) analysis. The STRING database (https://cn.string-db.org/) was used to analyze human genetic data and extract PPI information. Interaction patterns were thoroughly analyzed, with the species set as "*Homo sapiens*" and a confidence threshold of 0.7.

2.2 Construction of the target PPI network A "drug – DC maturation – target" interaction network was built utilizing molecular interaction data from the STRING database (https://string-db.org/). The 20 identified genes were imported into STRING to establish a PPI network, which was subsequently visualized and analyzed using Cytoscape software (version 3.9.0). In the visualizations, node size and color indicated degree values, with larger nodes denoting higher degrees. Edge thickness was proportional to the combined score, with thicker edges indicating higher scores. The final network was constructed based on core targets.

2.2.1 Molecular docking of ginsenoside Rh2 with pathway-related targets. To determine the structure of Rh2, the study retrieved its three-dimensional structure (Mol2 format) from the PubChem database (http://www.ncbi.nlm.nih.gov/). Crystal structures of potential target proteins were acquired from the Protein Data Bank (PDB, http://www.rcsb.org/). Structural processing was performed with PyMOL (version 2.4.0), along with molecular docking conducted using AutoDock Vina. Docking results were assessed by free binding energy, with values below −5.0 kJ/mol indicating strong interactions. Lower binding energy values corresponded to more stable docking complexes. The docking result with the lowest energy was selected for further analysis.

2.2.2 Molecular dynamics simulation of ginsenoside Rh2 with pathway-related targets. To clarify the atomic-level binding mechanism of Rh2, molecular dynamics simulations were conducted. Initially, the optimal complex from docking was immersed in a water box, followed by energy minimization and equilibration. A 200 ns production simulation was carried out under the NPT ensemble at 310 K and 1 bar. Trajectory analysis indicated that the complex remained stable throughout the simulation. Further analysis showed that Rh2 interacted with key amino acid residues through stable hydrogen bonds and hydrophobic interactions. MM-PBSA calculations confirmed a strong binding affinity. These simulations provided dynamic insights into the binding mode and stabilization mechanism of Rh2 at the atomic level.

2.2.3 Instruments and reagents. Instruments: Real-time fluorescence quantitative PCR system (QuantStudio™ 3, Thermo Fisher Scientific); inverted biological microscope (DMI1, Leica); low-speed desktop centrifuge (TDZ4-WS, Changsha Xiangyi Centrifuge Instrument Co., Ltd.); high-speed microcentrifuge (D3024, DragonLab Xingchuang Experimental Instrument Co., Ltd.); microplate reader (ELx800, BioTek Instruments, Inc.); flow cytometer (Cytoflex, Suzhou Celegene Biological Technology Co., Ltd.); and CO_2 incubator (311, Thermo Fisher Scientific).

Reagents: Total RNA Extraction Kit (100T, BL1365A, Biosharp Biotechnology Co., Ltd.); RNA Extraction Auxiliary Reagent (100 mL, BL1665A, Biosharp Biotechnology Co., Ltd.); anhydrous ethanol (analytical grade, Sinopharm Chemical Reagent Co., Ltd.); β-actin primary antibody (AC026, Abclonal); PDK1 primary antibody (A8930, Abclonal); PIK3R1 primary antibody (AF6241, Abclonal); PrimeScript™ RT Reagent Kit with gDNA Eraser (RR047A, Takara Bio Inc.); TB Green Premix Ex Taq™ II FAST qPCR Kit (CN830A, Takara Bio Inc.); and Ginsenoside Rh2 (BZP0241-20 mg, HPLC purity ≥ 98%, BIOBOMEI). Fig. 2A illustrates the molecular structure of ginsenoside Rh2.

2.3 Construction of breast cancer-bearing mouse model Sixty specific pathogen-free (SPF) female BALB/c mice [6 – 8 weeks old, weighing (20 ± 2) g] were obtained from SPF Biotechnology (Beijing, China; animal production license No.: SCXK [Beijing] 2024-0001; animal use license No.: SYXK [Sichuan] 2024-0287). The mice were housed under barrier conditions (temperature: 20 – 26 ℃, relative humidity: 30% – 70%, 12 h light/dark cycle) with free access to food and water. The study protocol was approved by the Ethics Committee of the Hospital of Traditional Chinese Medicine in Qijiang District.

After an initial adaptation period of 1 d, mice were housed 5 per cage. Following one week of adaptive feeding, each mouse was administered 0.1 mL of 4T1 mouse breast cancer cell suspension (approximately 1×10^6 cells) by subcutaneous injection into the axilla to establish a subcutaneous breast cancer xenograft model. The general condition of mice (mental state, activity, hair luster, fecal characteristics, and urination) was monitored daily at fixed times throughout the experimental period. Body weight was measured weekly, and tumor diameter was recorded every 3 d after tumor formation. When tumors reached approximately 200 mm^3, mice were anesthetized with 1% pentobarbital sodium (50 mg/kg) administered via intraperitoneal injection. After confirming unconsciousness (no response to toe compression), mice were sacrificed by bloodletting and cervical dislocation. Following confirmation of cardiac and respiratory arrest, mice were immersed in 75% ethanol for 10 min, and femurs and tibias were collected aseptically.

2.3.1 Isolation and induction of BMDCs. The femurs and tibias of mice were collected aseptically and rinsed twice with 1 × PBS. The bone ends were cut, and the marrow was flushed repeatedly

with PBS using a 1 mL syringe until the bones turned white. The cell suspension was filtered through a 200 mesh cell strainer to remove debris and collected into a 15 mL centrifuge tube. After centrifugation, red blood cells were lysed using red blood cell lysis buffer, and the reaction was terminated with PBS. The cells were centrifuged again, washed twice, and resuspended in RPMI 1640 complete medium containing recombinant mouse GM-CSF (20 ng/mL) and IL-4 (10 ng/mL). The cells were then cultured in an incubator for 7 d to induce differentiation into immature dendritic cells (iDCs).

2.3.2 Flow cytometry for surface marker detection. DCs were adjusted to 2×10^5 cells/well, seeded into 6-well plates (2 mL/well), and cultured for a specified duration at 37 ℃ in a 5% CO_2 incubator. After 24 h of treatment according to the experimental groups, cell suspensions were collected and centrifuged for 5 min at 250 × g, with supernatants discarded. Cells were washed with PBS, transferred to 1.5 mL conical EP tubes, centrifuged again (250 × g, 5 min), and the supernatants were discarded. The cells were resuspended in 100 μL of PBS and incubated with the corresponding antibodies (CD11b, CD11c, MHC-II, CD80, CD86) for 30 min at 4 ℃ in the dark. Subsequent to centrifugation at 300 × g for 5 min , the cells were washed once, resuspended in 300 μL of PBS, and analyzed using a flow cytometer.

2.4 Cell grouping and treatment After washing with PBS, iDCs in the logarithmic growth phase were digested with trypsin and centrifuged at 250 × g for 5 min. The cells were resuspended in medium to prepare a single-cell suspension (5×10^5 cells/mL). The suspension was then seeded into 6-well plates (2 mL/well). After adherence, two treatment protocols were conducted: (i) Protocol 1: iDC group; iDC + LPS (1 μg/mL) group; iDC + low-dose Rh2 (0.625 μg/mL) group; iDC + high-dose Rh2 (6.25 μg/mL) group; iDC + LPS + low-dose Rh2 group; and iDC + LPS + high-dose Rh2 group. Treatments were applied for 24 h. (ii) Protocol 2: iDC group; iDC + ov-NC (empty vector control) group; iDC + ov-PIK3R1 (PIK3R1 overexpression) group; iDC + Rh2 group; and iDC + Rh2 + ov-PIK3R1 group. The cells were transfected accordingly and treated with high-dose Rh2 for 24 h.

2.4.1 Cell transfection. Two 1.5 mL centrifuge tubes were prepared, each containing 300 μL of Opti-MEM™ I medium. One tube received 15 μg of plasmid, and the other received 30 μL of Lipofectamine 2000 transfection reagent. The solutions were gently mixed and allowed to stand for 5 min, followed by a combined incubation for another 10 min. The medium was added to reach a total volume of 6 mL. Cells (2×10^5 cells/mL) were seeded into 6-well plates (2 mL/well) and cultured at 37 ℃, 5% CO_2 for a specified period. After cell adherence, the supernatants were replaced with the transfection complexes. The cells were then incubated for 6 h at 37 ℃ and 5% CO_2, after which the medium was replaced with complete medium.

2.4.2 CCK-8 cell viability assay. DCs were seeded into 96-well plates at a density of 5×10^4 cells/mL (100 μL/well)). The marginal wells were filled with sterile PBS. After incubation at 37 ℃ with 5% CO_2, the cells were treated for 24, 48, and 72 h with varying concentrations of ginsenoside Rh2 (0, 6.25, 12.5, 25, 50, 100, 200, and 400 μg/mL), with four replicates per group. Following treatment, the supernatant was removed, and 110 μL of CCK-8 reagent (diluted 1∶10 with serum-free medium) was added to each well. The plates were gently shaken and incubated for another 2 h at 37 ℃, 5% CO_2. Absorbance was measured at 450 nm using a microplate reader to calculate cell viability.

2.4.3 ELISA for inflammatory cytokine detection. The collected cell culture supernatants were analyzed using ELISA. The kit was equilibrated to room temperature for 30 min, and the necessary plate strips were removed from the foil packaging. Standard and sample wells were prepared by adding 50 μL of standards or samples, while blank wells were left empty. Except for the blank wells, each well was added with 100 μL of HRP-labeled detection antibody. The plates were sealed and incubated for 60 min at 37 ℃. After discarding the liquid, the plates were washed 5 times with washing solution. Each well was added with substrates A and B (50 μL each) and incubated for 15 min at 37 ℃ in the dark. 50 μL of stop solution was added, and absorbance (OD) was measured at 450 nm within 10 min.

2.4.4 Western blotting (WB) for pathway protein expression. Total protein was extracted using RIPA lysis buffer, and concentrations were quantified by BCA assay. After denaturation, proteins were separated by SDS-PAGE and transferred onto PVDF membranes. Subsequent to 1 h of blockage in 5% non-fat milk, membranes were incubated overnight at 4 ℃ with primary antibodies: PDK1 (1∶10 000), PIK3R1 (1∶2 000), and β-actin (1∶50 000). This was followed by a 1 h incubation at room temperature with an HRP-conjugated goat anti-rabbit secondary antibody (1∶8 000). Protein bands were visualized using ECL reagent and analyzed by an automated chemiluminescence imaging system. Band intensities (IOD) were quantified using Gel-Pro Analyzer 4 software.

2.4.5 RT-PCR for gene expression detection. A total RNA extraction kit was employed to isolate total RNA from cells. Genomic DNA was removed by incubation at 42 ℃ for 2 min, followed by reverse transcription into cDNA at 37 ℃ for 15 min and 85 ℃ for 5 sec, according to the kit instructions. PCR amplification was conducted using a real-time PCR instrument. The primers used are listed in Table 1. Relative mRNA expression levels were calculated using the $2^{-\Delta\Delta Ct}$ method.

Table 1 Primers and base sequences used in this study

Gene	Forward (5'→3')	Reverse (5'→3')	Amplicon length//bp
β-actin	ctacctcatgaagatcctgacc	cacagcttctctttgatgtcac	90
PDK1	cttagagggctacgggacagatg	atgcttccaggcggctttattg	100
PIK3R1	acagtaggaggaggttggaagaag	tgcgtcagccacatcaagtattg	139

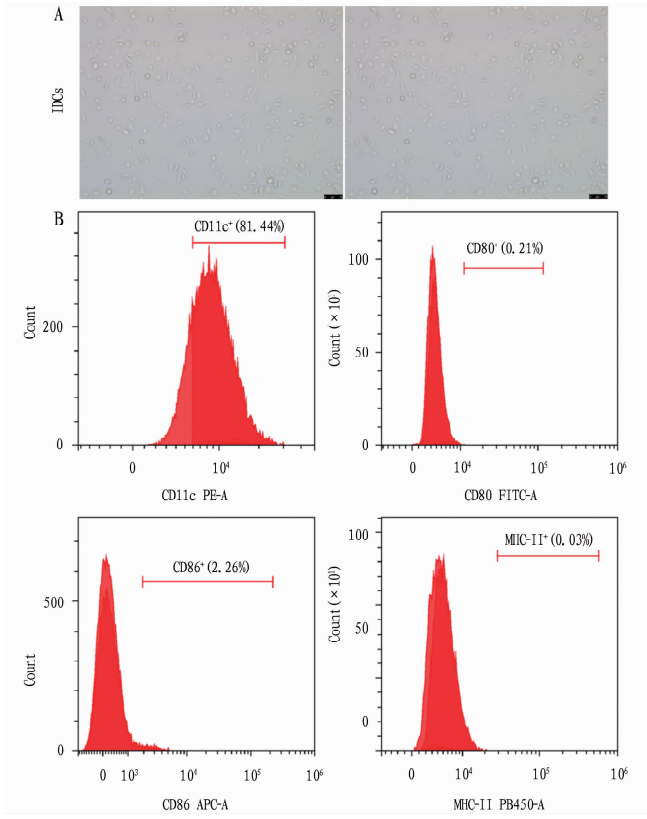
2.5 Statistical analysis Experimental data are expressed as mean ± standard deviation (SD). Statistical analyses were per-

formed using SPSS 20.0 software. Between-group difference was analyzed by one-way ANOVA, and pairwise comparisons used the least significant difference (*LSD*) test. $P<0.05$ denoted statistical significance.

3 Results and analysis

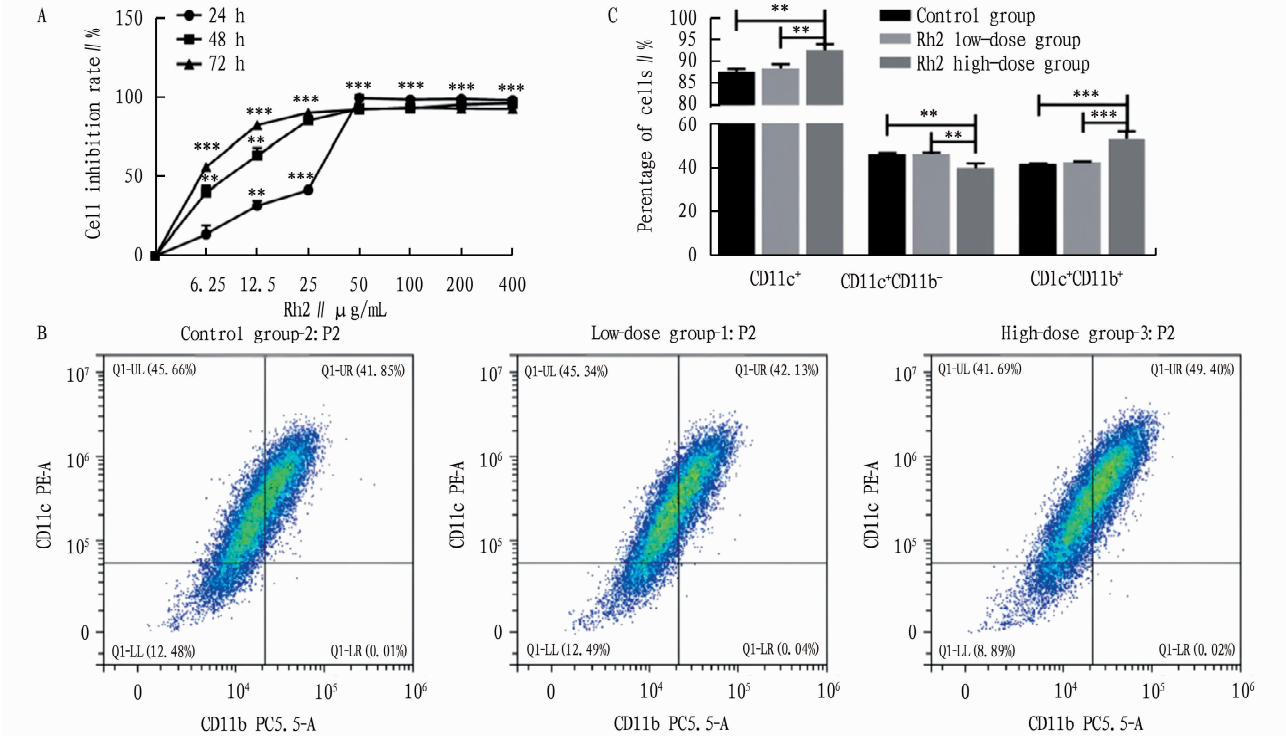
3.1 Isolation, induction, and identification of BMDCs from breast cancer-bearing mice During cell culture, obvious morphological alterations were detected under an inverted microscope, showing the typical irregular shapes and protrusions characteristic of DCs (Fig. 1A). Flow cytometry analysis confirmed that the expression rate of $CD11c^+$ cells in the induced population was as high as 80.68% ±0.76%, while the expression rates of $CD80^+$, $CD86^+$, and $MHC\text{-}II^+$ were low, at 0.22% ±0.04%, 2.38% ± 0.15%, and 0.02% ±0.01%, respectively (Fig. 1B). This phenotype (high CD11c expression, low costimulatory molecule and MHC-II expression) matches the characteristics of iDCs, confirming successful isolation and induction from mouse bone marrow.

3.2 Effect of ginsenoside Rh2 on BMDC differentiation To evaluate the effect of Rh2 on BMDC function in breast cancer models, dose- and time-dependent effects on cell viability were first assessed. Cells were treated with Rh2 (0, 6.25, 12.5, 25, 50, 100, 200, 400 μg/mL) for 24, 48, and 72 h, and cell viability was measured with the CCK-8 assay. Rh2 significantly inhibited cell viability at concentrations of 12.5 μg/mL and above after 24 h ($P<0.01$, Fig. 2A). Therefore, a low dose (0.625 μg/mL) and a high dose (6.25 μg/mL) of Rh2 with a 24 h treatment were selected for subsequent experiments.



NOTE A. Morphological changes of cells observed under an inverted microscope; B. Flow cytometric detection of DC markers: CD11c, MHC-II, CD80, and CD86.

Fig. 1 Identification of BMDCs



NOTE A. CCK-8 assay detection of cell viability; B – C. Flow cytometric detection of CD11c and CD11b. $^{**}P<0.01$, $^{***}P<0.001$.

Fig. 2 Effect of ginsenoside Rh2 on BMDC differentiation from breast cancer models

Mouse bone marrow cells cultured with rmGM-CSF (20 ng/mL) and rmIL-4 (10 ng/mL) were treated with Rh2 (low and high doses) or left untreated for 7 d. The proportions of CD11c and CD11b expressing cells were analyzed via flow cytometry (Fig. 2B – C). The proportion of $CD11c^+$ cells significantly increased in the high-dose Rh2 group compared to the control ($P<0.01$), suggesting that Rh2 promotes DC differentiation. Additionally, the proportion of $CD11c^+CD11b^+$ cells increased, while the proportion of $CD11c^+CD11b^-$ cells correspondingly decreased in the high-dose group ($P<0.01$). This phenotypic change suggests that Rh2 preferentially stimulates differentiation toward cDC2-like cells. Collectively, these results indicate that ginsenoside Rh2 enhances overall DC differentiation and affects the balance between cDC1 ($CD11b^-$) and cDC2 ($CD11b^+$) subsets through subset-specific pathways.

3.3 Effect of ginsenoside Rh2 on BMDC maturation in breast cancer models To further explore the effect of Rh2 on DC maturation, BMDCs were treated with various concentrations of Rh2 , either alone or in combination with LPS (1 μg/mL) to induce maturation. Flow cytometry results (Fig. 3 A – B) demonstrated significant increases in the populations of $CD11c^+CD80^+$ and $CD11c^+MHC\text{-}II^+$ cells in the LPS alone, low-dose Rh2, and high-dose Rh2 groups compared to controls ($P<0.05$). The proportion of $CD11c^+CD86^+$ cells showed an obvious elevation in the LPS and low-dose Rh2 groups ($P<0.05$) but not in the high-dose Rh2 group ($P>0.05$), suggesting potential signal saturation or feedback inhibition at higher Rh2 doses. Synergistic analysis showed that combining LPS with low-dose Rh2 significantly increased the proportions of $CD11c^+CD80^+$, $CD11c^+CD86^+$, and $CD11c^+MHC\text{-}II^+$ cells compared to Rh2 alone ($P<0.001$), indicating a synergistic effect between low-dose Rh2 and LPS. The combination of LPS with high-dose Rh2 significantly enhanced the proportions of $CD11c^+CD80^+$ and $CD11c^+CD86^+$ cells ($P<0.001$) but did not significantly affect $CD11c^+MHC\text{-}II^+$ cells ($P>0.05$), possibly due to inhibitory effects on specific pathways. Furthermore, compared to LPS alone, combinations of LPS with either low- or high-dose Rh2 significantly increased the proportions of $CD11c^+CD80^+$ and $CD11c^+CD86^+$ cells ($P<0.001$), while $CD11c^+MHC\text{-}II^+$ cells increased significantly only with low-dose Rh2 ($P<0.001$). These findings demonstrate dose-dependent effects of Rh2 on DC surface marker expression and suggest that Rh2 promotes DC maturation both independently and synergistically with LPS.

Fig. 3C illustrates the cytokine secretion results. Compared to the control group, treatments with LPS alone, low-dose Rh2, and high-dose Rh2 remarkably stimulated the secretion of the pro-inflammatory cytokines IL-12 and TNF-α, while inhibiting the anti-inflammatory cytokine IL-10 ($P<0.05$). Compared to Rh2 alone, combinations of LPS with either low- or high-dose Rh2 synergistically enhanced IL-12 and TNF-α secretion and further inhibited IL-10 ($P<0.05$). Similarly, relative to LPS alone, the addition of Rh2 (at either dose) significantly enhanced the expression of IL-12 and TNF-α and lowered IL-10 levels ($P<0.05$).

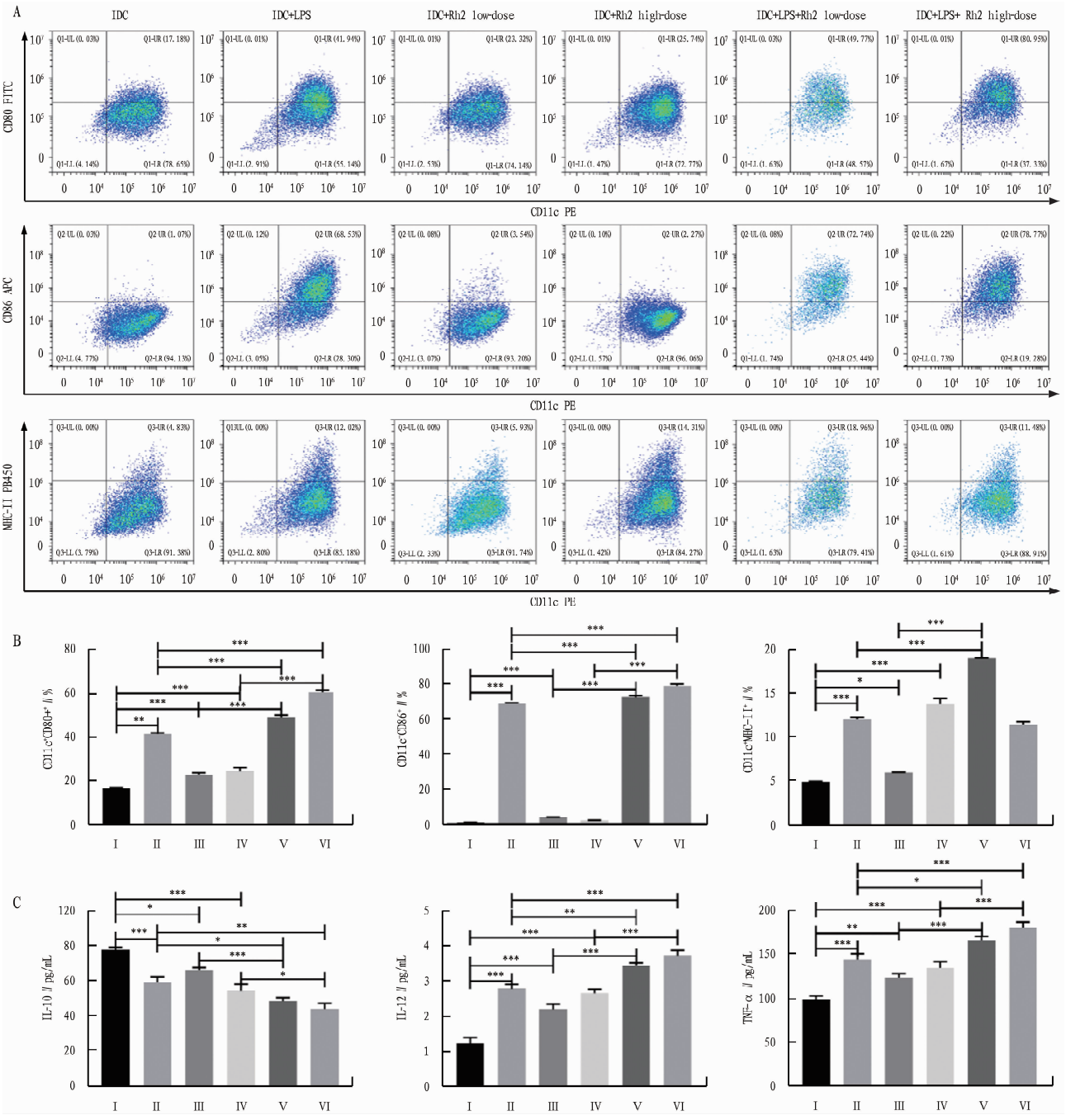
These findings indicate that ginsenoside Rh2, either alone or in combination with LPS, promotes DC maturation and induces a pro-inflammatory activation state. This conclusion is supported by the increased expression of key co-stimulatory molecules (CD80, CD86) and MHC-II, along with polarization toward a pro-inflammatory cytokine profile.

3.4 Effect of ginsenoside Rh2 on the PIK3R1-PDK1 pathway in BMDCs from breast cancer models To investigate the molecular mechanisms underlying Rh2-induced DC maturation, a "drug-DC maturation-target" regulatory network was established using network pharmacology (Fig. 4). This analysis identified 20 potential target genes involved in Rh2-mediated DC maturation. Among these, PIK3R1 occupied a key position in the network, suggesting its crucial role in the process.

Subsequently, the expression levels of molecules related to the PIK3R1-PDK1 pathway were measured by WB and RT-PCR (Fig. 5). Compared to the control group, treatment with LPS alone, low-dose Rh2, and high-dose Rh2 significantly inhibited the protein expression of PIK3R1 and PDK1 ($P<0.05$, Fig. 5A – B). Additionally, combinations of LPS and Rh2 (low or high dose) further suppressed the protein expression of these molecules compared to single-agent treatments ($P<0.05$, Fig. 5A – B). The gene expression results were consistent with the protein data: both single treatments (LPS alone, low-dose Rh2, high-dose Rh2) and combined treatments (LPS + Rh2) significantly downregulated PIK3R1 and PDK1 mRNA expression ($P<0.05$, Fig. 5C). According to the above findings, at both the protein and gene levels, ginsenoside Rh2, either alone or in combination with LPS, significantly inhibits activation of the PIK3R1-PDK1 pathway in BMDCs from breast cancer models.

3.5 Ginsenoside Rh2 promotes BMDC maturation via the PIK3R1-PDK1 pathway To clarify the role of the PIK3R1-PDK1 pathway in Rh2-induced DC maturation, a PIK3R1 overexpression plasmid (ov-PIK3R1) was constructed and transfected into BMDCs. WB results (Fig. 6A – B) showed that Rh2 significantly reduced PIK3R1 and PDK1 protein expression ($P<0.05$), consistent with previous findings. Overexpression of PIK3R1 significantly increased the protein levels of PIK3R1 and PDK1, reversing the Rh2-induced suppression ($P<0.001$). The empty vector (ov-NC) had no significant effect ($P>0.05$). RT-PCR results mirrored these protein expression trends (Fig. 6C): ov-PIK3R1 significantly increased the mRNA expression levels of PIK3R1 and PDK1, and reversed the reductions induced by Rh2 ($P<0.05$).

Further analysis indicated that neither Rh2 nor ov-PIK3R1 alone influenced cell viability ($P>0.05$, Fig. 7A). Flow cytometry revealed that Rh2 significantly increased proportions of $CD11c^+CD80^+$ and $CD11c^+MHC\text{-}II^+$ cells ($P<0.001$, Fig. 7B – C), confirming its effect in promoting DC maturation. However, PIK3R1 overexpression (ov-PIK3R1 group) significantly decreased the

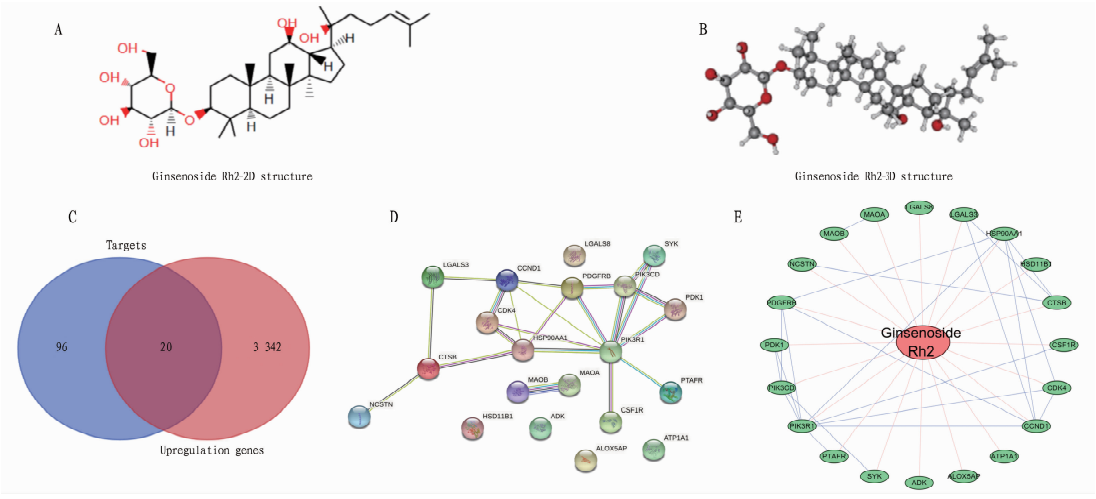


NOTE A. Representative flow cytometry plots showing the expression of surface markers (CD80, CD86, MHC-II) on BMDCs in each treatment group; B. Statistical bar graphs illustrating percentages of $CD11c^+CD80^+$, $CD11c^+CD86^+$, and $CD11c^+MHC\text{-}II^+$ cells; C. Levels of IL-12, TNF-α, and IL-10 in cell supernatants measured by ELISA. Groups: I. IDC; II. IDC + LPS; III. IDC + Rh2 low-dose; IV. IDC + Rh2 high-dose; V. IDC + LPS + Rh2 low-dose; VI. IDC + LPS + Rh2 high-dose. $^*P<0.05$, $^{**}P<0.01$, $^{***}P<0.001$.

Fig 3 Effect of ginsenoside Rh2 on BMDC maturation in breast cancer models

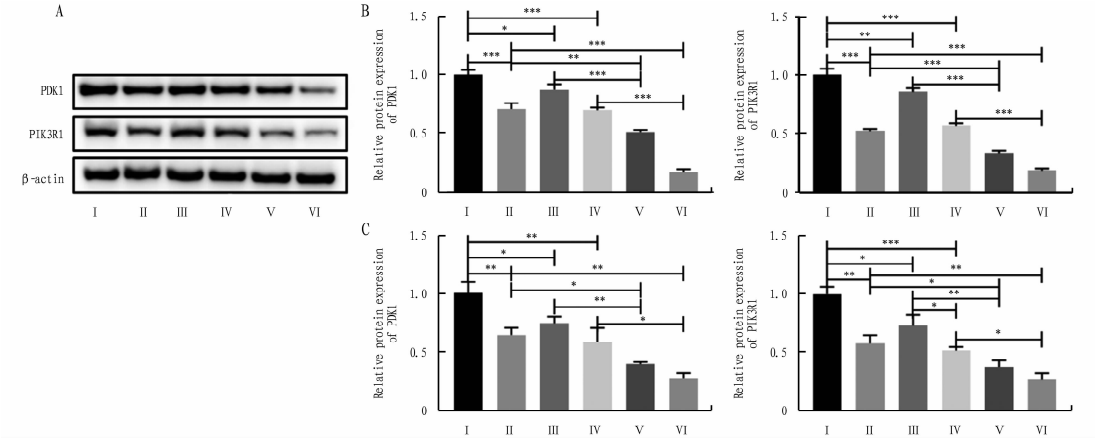
proportion of $CD11c^+CD80^+$ cells ($P<0.001$) and slightly increased $CD11c^+MHC\text{-}II^+$ cells ($P<0.05$), indicating differential regulatory effects on maturation markers. Critically, co-treatment with Rh2 and ov-PIK3R1 significantly reversed the Rh2-induced increase in $CD11c^+MHC\text{-}II^+$ cells ($P<0.001$), and also decreased the proportion of $CD11c^+CD80^+$ cells, although this decrease was not statistically significant ($P>0.05$). These findings suggest that PIK3R1 overexpression can counteract the effects of Rh2 on DC maturation.

These results confirm that the PIK3R1-PDK1 pathway serves as a key negative regulatory mechanism in Rh2-induced DC maturation. In summary, ginsenoside Rh2 promotes DC maturation in breast cancer-bearing mice primarily by inhibiting the PIK3R1-PDK1 signaling pathway (Fig. 8).



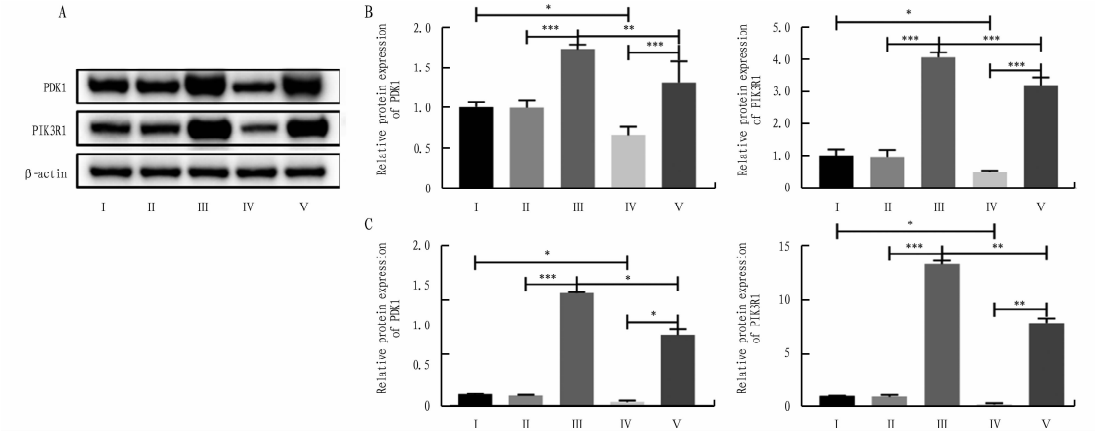
NOTE A – B. 2D and 3D chemical structures of ginsenoside Rh2; C. Venn diagram demonstrating the intersection between predicted Rh2 targets (SwissTargetPrediction platform) and highly expressed genes in immature DCs (GEO dataset GSE15076) for identifying key genes; D. PPI network of the 20 identified genes built utilizing the STRING database; E. "Drug-DC maturation-target" regulatory network.

Fig. 4 Potential mechanisms of ginsenoside Rh2-mediated DC maturation predicted by network pharmacology



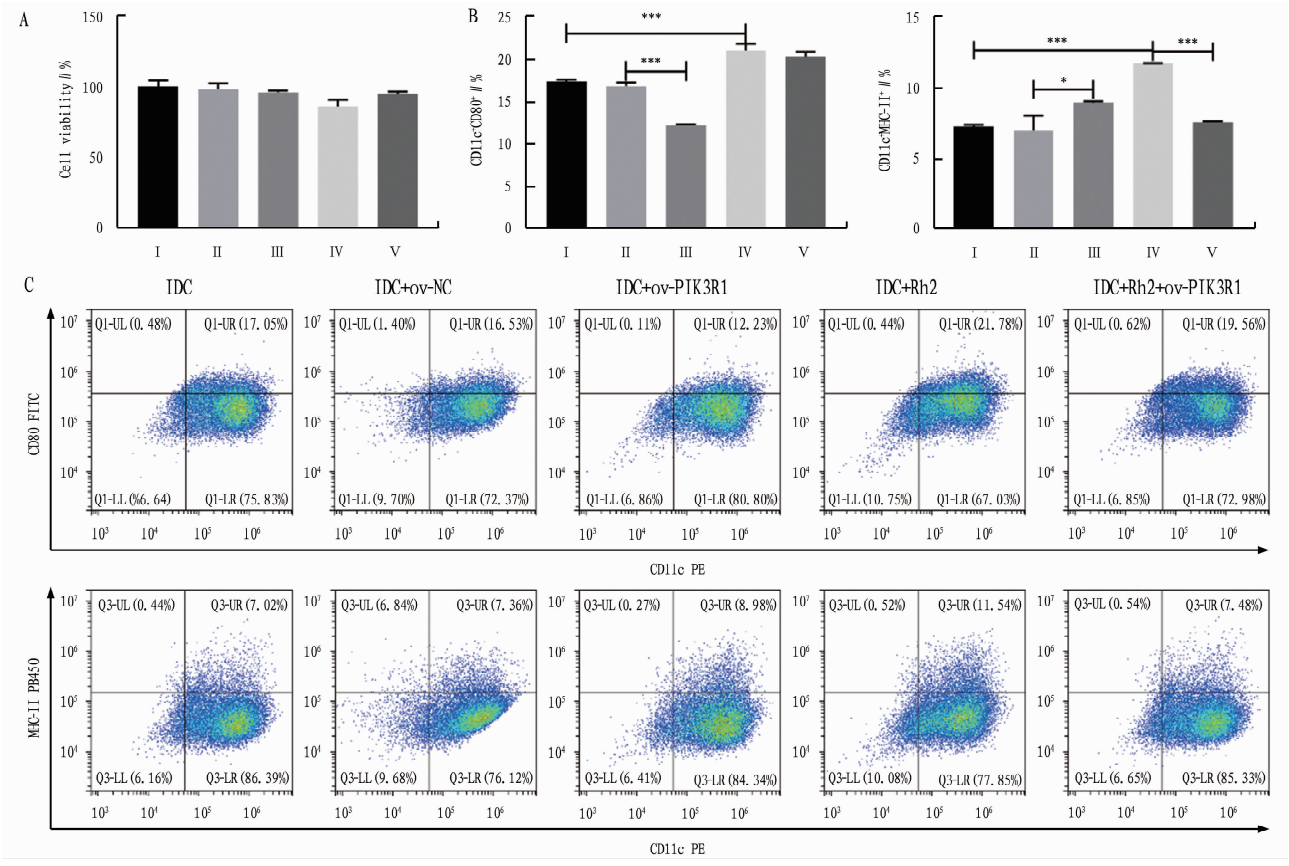
NOTE A. WB images showing PIK3R1 and PDK1 protein expression; B. Statistical analysis of relative protein expression levels of PIK3R1 and PDK1; C. Relative mRNA expression levels of PIK3R1 and PDK1 under RT-PCR measurement. Groups: I. IDC; II. IDC + LPS; III. IDC + Rh2 low-dose; IV. IDC + Rh2 high-dose; V. IDC + LPS + Rh2 low-dose; VI. IDC + LPS + Rh2 high-dose. $^{*}P<0.05$, $^{**}P<0.01$, $^{***}P<0.001$.

Fig. 5 Ginsenoside Rh2 inhibits activation of the PIK3R1-PDK1 pathway in BMDCs from breast cancer models



NOTE A. WB images of PIK3R1 and PDK1 proteins; B. Statistical analysis of relative protein expression levels; C. Relative mRNA expression levels of PIK3R1 and PDK1 under RT-PCR detection. Groups: I. IDC; II. IDC + ov-NC; III. IDC + ov-PIK3R1; IV. IDC + Rh2; V. IDC + Rh2 + ov-PIK3R1. $^{*}P<0.05$, $^{**}P<0.01$, $^{***}P<0.001$.

Fig. 6 Expression of the PIK3R1-PDK1 pathway in BMDCs following PIK3R1 overexpression



NOTE A. CCK-8 assay assessment of cell viability; B – C. Flow cytometry analysis of BMDC surface markers ($CD11c^+CD80^+$ and $CD11c^+MHC\text{-}II^+$). Groups: I. IDC; II. IDC + ov-NC; III. IDC + ov-PIK3R1; IV. IDC + Rh2; V. IDC + Rh2 + ov-PIK3R1. $^*P<0.05$, $^{**}P<0.01$, $^{***}P<0.001$.

Fig. 7 Effect of PIK3R1 overexpression on Rh2-induced BMDC maturation in breast cancer models

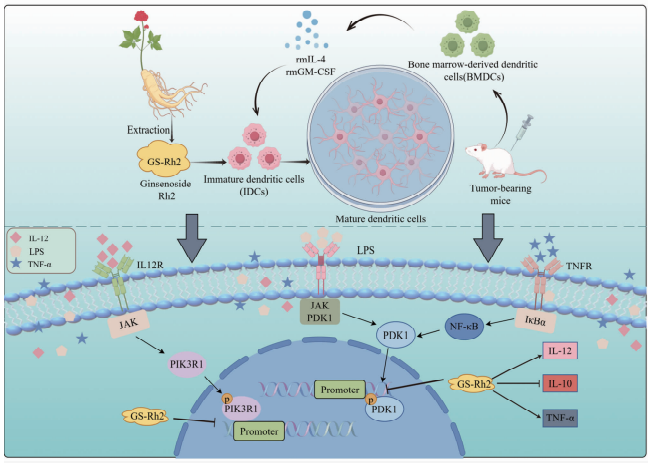


Fig. 8 Schematic representation of GS-Rh2 effects on the PIK3R1-PDK1 signaling pathway (created with Figdraw)

4 Discussion

This study provides robust evidence that ginsenoside Rh2, a bioactive compound derived from ginseng, promotes the maturation of BMDCs in a breast cancer mouse model by primarily inhibiting the PIK3R1-PDK1 signaling pathway. These findings enhance our understanding of the immunomodulatory and anti-tumor mechanisms of ginsenoside Rh2, offering new perspectives and suggesting potential applications in breast cancer immunotherapy.

DCs are critical regulators of adaptive immune responses, especially in tumor immunology[23-25]. The maturation status of DCs directly influences the efficacy of anti-tumor immune responses[26-27]. In this study, Rh2 significantly increased the expression of DC maturation markers (CD80, CD86, MHC-II) and induced a pro-inflammatory cytokine profile (increased IL-12 and TNF-α, decreased IL-10) in BMDCs. Importantly, Rh2 demonstrated synergistic effects with LPS, a classical inducer of DC maturation, further enhancing DC maturation and activation. These results suggest that Rh2 could serve as an adjuvant to strengthen DC-based immunotherapies.

Network pharmacology identified PIK3R1 as the central node within the "drug-DC maturation-target" network, highlighting its potential role in mediating the effects of Rh2. Subsequent experiments confirmed that Rh2 reduced both the mRNA and protein expression levels of PIK3R1 and its downstream effector PDK1. The PIK3R1-PDK1 axis is an essential upstream regulator of the PI3K/AKT pathway, which modulates cell survival, proliferation, and immune functions[28-30]. Rh2-mediated inhibition of this pathway may alleviate inhibitory signals that restrict DC maturation within the tumor microenvironment[31-32].

Functional rescue experiments further validated the causal re-

lationship between the inhibition of PIK3R1-PDK1 pathway and Rh2-induced DC maturation, as overexpression of PIK3R1 reversed the effects of Rh2. Interestingly, PIK3R1 overexpression alone showed differential effects on DC maturation markers: it slightly enhanced MHC-II expression but inhibited CD80 expression. These findings underscore the complexity of PIK3R1 signaling in DC biology, indicating that precise modulation of this pathway may differentially affect specific DC functions.

Compared to traditional chemotherapeutic agents, Rh2 exhibited a favorable safety profile, exhibiting no significant cytotoxicity at effective doses. This finding aligns with the growing emphasis on natural compounds as safer adjuvants or alternatives to conventional therapies, aiming to reduce off-target toxicity and improve clinical outcomes in cancer treatment[33-34].

Nevertheless, this study has several limitations. First, the research primarily relied on a mouse breast cancer model and *in vitro* DC cultures. The translational relevance to human breast cancer and primary human DCs needs further validation. Second, although the current study focused on the PIK3R1-PDK1 axis, other pathways and molecular targets identified through network analysis may also mediate the immunomodulatory effects of Rh2. Further studies using multi-omics and *in vivo* validation are required to fully elucidate the comprehensive mechanisms of Rh2. Finally, the long-term therapeutic efficacy of Rh2 and its potential combinations with existing immunotherapies, such as immune checkpoint inhibitors, shall be well elucidated.

5 Conclusions

To sum up, this study demonstrates that ginsenoside Rh2 promotes DC maturation and functional activation in breast cancer models by inhibiting the PIK3R1-PDK1 signaling pathway. These findings reveal a previously unrecognized immunomodulatory mechanism of Rh2 and highlight its potential as a natural adjuvant to enhance anti-tumor immunity. This work provides a theoretical foundation for the application of Rh2 in DC-based immunotherapy, contributing to the development of novel and low-toxicity therapeutic strategies for breast cancer. Future clinical studies shall be conducted to verify these preclinical findings and evaluate the translational potential of ginsenoside Rh2 in oncology.

References

[1] PRADIPTA AR, TANEI T, MORIMOTO K, *et al.* Emerging technologies for real-time intraoperative margin assessment in future breast-conserving surgery[J]. Advanced Science, 2020, 7(9): 1901519.

[2] CHOI JE, KIM Z, PARK CS, *et al.* Breast cancer statistics in Korea, 2019[J]. Journal of Breast Cancer, 2023, 26(3): 207-220.

[3] BRAUN B, KHIL L, TIO J, *et al.* Differences in breast cancer characteristics by mammography screening participation or non-participation[J]. Deutsches Ärzteblatt International, 2018, 115(31-32): 520-527.

[4] MATUSCHEK C, JAZMATI D, BÖLKE E, *et al.* Post-neoadjuvant treatment strategies in breast cancer[J]. Cancers, 2022, 14(5): 1246.

[5] PASHAYAN N, ANTONIOU AC, IVANUS U, *et al.* Personalized early detection and prevention of breast cancer: ENVISION consensus statement [J]. Nature Reviews Clinical Oncology, 2020, 17: 687-705.

[6] PASSARO A, AL BAKIR M, HAMILTON EG, *et al.* Cancer biomarkers: Emerging trends and clinical implications for personalized treatment [J]. Cell, 2024, 187(7): 1617-1635.

[7] RUHSTALLER T, GIOBBIE-HURDER A, COLLEONI M, *et al.* Adjuvant letrozole and tamoxifen alone or sequentially for postmenopausal women with hormone receptor-positive breast cancer: Long-term follow-up of the BIG 1-98 trial[J]. Journal of Clinical Oncology, 2019, 37(2): 105-114.

[8] LEE KM, GUERRERO-ZOTANO AL, SERVETTO A, *et al.* Proline rich 11 (PRR11) overexpression amplifies PI3K signaling and promotes antiestrogen resistance in breast cancer[J]. Nature Communications, 2020, 11(1): 5488.

[9] NIKOO M, RUDIANSYAH M, BOKOV DO, *et al.* Potential of chimeric antigen receptor (CAR)-redirected immune cells in breast cancer therapies: Recent advances[J]. Journal of Cellular and Molecular Medicine, 2022, 26(15): 4137-4156.

[10] VOROBYEVA A, BEZVERKHNIAIA E, KONOVALOVA E, *et al.* Radionuclide molecular imaging of EpCAM expression in triple-negative breast cancer using the scaffold protein DARPin Ec1[J]. Molecules, 2020, 25(20): 4719.

[11] SANKARANARAYANAN RA, PEIL J, VOGG ATJ, *et al.* Auger emitter conjugated PARP inhibitor for therapy in triple negative breast cancers: A comparative *in-vitro* study[J]. Cancers, 2022, 14(1): 230.

[12] WANG Q, KARVELSSON ST, JOHANNSSON F, *et al.* UDP-glucose dehydrogenase expression is upregulated following EMT and differentially affects intracellular glycerophosphocholine and acetylas partate levels in breast mesenchymal cell lines[J]. Molecular Oncology, 2022, 16(9): 1816-1840.

[13] MAHMOUD R, ORDÓÑEZ-MORÁN P, ALLEGRUCCI C. Challenges for triple negative breast cancer treatment: defeating heterogeneity and cancer stemness[J]. Cancers, 2022, 14(17): 4280.

[14] WEI C, LU Y, QIU L, *et al.* Designing personalized treatment plans for breast cancer[J]. Information Systems Research, 2021, 32(3): 932-949.

[15] Kang ZP, Zhonga YB, Wu TT, *et al.* Ginsenoside from ginseng: A promising treatment for inflammatory bowel disease[J]. Pharmacological Reports, 2021, 73(3): 700-711.

[16] VALDÉS-GONZÁLEZ JA, SÁNCHEZ M, MORATILLA-RIVERA I, *et al.* Immunomodulatory, anti-inflammatory, and anti-cancer properties of ginseng: A pharmacological update[J]. Molecules, 2023, 28(9): 3863.

[17] PIAO XM, HUO Y, KANG JP, *et al.* Diversity of ginsenoside profiles produced by various processing technologies[J]. Molecules, 2020, 25 (19): 4390.

[18] JI YJ, KIM HD, LEE ES, *et al.* Heat treatment enhances the neuroprotective effects of crude ginseng saponin by increasing minor ginsenosides [J]. International Journal of Molecular Sciences, 2023, 24(8): 7223.

[19] HONG CE, LYU SY. Immunomodulatory activities of emerging rare ginsenosides F1, Rg5, Rk1, Rh1, and Rg2: From molecular mechanisms to therapeutic applications[J]. Pharmaceuticals, 2025, 18(10): 1529.

[20] BAE J, KOO J, KIM S, *et al.* Ginsenoside Rp1 exerts anti-inflammatory effects via activation of dendritic cells and regulatory T cells[J]. Journal of Ginseng Research, 2012, 36(4): 375.

[21] ZHANG H, PARK S, HUANG H, *et al.* Anticancer effects and potential mechanisms of ginsenoside Rh2 in various cancer types (Review) [J]. Oncology Reports, 2021, 45: 33.

[22] LIU S, CHEN W, ZHAO Y, *et al.* Research progress on effects of ginsenoside Rg2 and Rh1 on nervous system and related mechanisms[J]. Molecules, 2023, 28(23): 7935.

(To page 38)

(2020 Edition, General Chapter 0502). Aliquots of 2 μL each of the test solution, negative control, and reference medicinal material solution were spotted onto the same plate. The plate was developed with a mixture of cyclohexane, ethyl acetate, and formic acid (13∶6∶1), removed, and air-dried. It was then sprayed with 10% sulfuric acid in ethanol and heated at 105 ℃ until the spots became clearly visible. The plate was examined under ultraviolet light at 365 nm. As shown in Fig. 3, the test solution exhibited fluorescent spots of the same color at positions corresponding to those in the reference medicinal material chromatogram.

4 Discussion

4.1 Rationality of the extraction process The water decoction method was chosen for this study not only to maintain consistency with the traditional decoction, but also to meet the requirements of industrial production. The orthogonal experimental results showed that extraction frequency was the key factor affecting both the dry extract yield and the transfer rates of the marker components ($P < 0.05$ or $P < 0.01$), whereas water addition amount and extraction time had no significant effects. With consideration for energy conservation and production cycle reduction, two decoction cycles were selected instead of three, reflecting a process design principle that prioritizes therapeutic efficacy while taking efficiency into account. Validation experiments confirmed that the process was stable and feasible, with all *RSD* values within acceptable limits.

4.2 Characteristics of the quality standard The established TLC identification method covers the three main medicinal materials (Lonicerae Japonicae Flos, Forsythiae Fructus, and Glycyrrhizae Radix et Rhizoma) with strong specificity, no interference from negative controls, and simple operation. It can serve as a qualitative control indicator for the preparation. The results of all inspection items met the requirements for oral liquids (mixtures) specified in the *Chinese Pharmacopoeia* (2020 Edition), and the microbial limits were within the prescribed standards, indicating that the quality of this preparation is controllable.

4.3 Future research prospects As the principal herb in the formula, *Clerodendrum japonicum* currently lacks a well-established TLC identification method. Further efforts are needed to explore more favorable conditions for extraction, separation, and development, so as to establish a highly specific TLC or HPLC identification method for this herb. In addition, it is recommended that quantitative studies be carried out on forsythiaside and chlorogenic acid, and that a multi-component quality standard be developed to provide a more comprehensive basis for the quality control of the preparation.

5 Conclusions

The optimal extraction process for Chengyin Mixture established in this study was as follows: decocting twice with 10 times the amount of water, one hour for each decoction. Validation experiments confirmed that the process was stable and feasible, with a mean dry extract yield of 24.24%, and mean transfer rates of 71.86% for forsythiaside and 69.48% for chlorogenic acid, all with *RSD* values below 5%. The TLC identification methods developed were highly specific with no interference from negative controls. The appearance, relative density, pH, filling volume, and microbial limits of the preparation all met the requirements of the *Chinese Pharmacopoeia*. This process and the associated quality standards can serve as a basis for the hospital preparation registration and standardized production of Chengyin Mixture.

References

[1] QIN ZJ, ZHANG M, SONG N. Clinical observation of efficacy on treatment of Chengyin Decoction for acute tonsillitis[J]. Chinese Journal of Experimental Traditional Medical Formulae, 2013, 19(12): 307 – 310. (in Chinese).

[2] WEI JC, CHEN Y, XIE Z, *et al*. Technology optimization and content determination of caffeic acid in 10 batches of laggera alata from different areas[J]. China Pharmacy, 2017, 28(34): 4792 – 4795. (in Chinese).

[3] WEI JC, CHEN Y, XIE Z, *et al*. TLC identification of Laggera alata and extraction process and content determination of chlorogenic acid[J]. Journal of Li-Shizhen Traditional Chinese Medicine, 2017, 28(11): 2611 – 2614. (in Chinese).

(From page 33)

[23] JOFFRE O, NOLTE MA, SPÖRRI R, *et al*. Inflammatory signals in dendritic cell activation and the induction of adaptive immunity[J]. Immunological Reviews, 2009, 227(1): 234 – 247.

[24] MELLMAN I. Dendritic cells: Master regulators of the immune response [J]. Cancer Immunology Research, 2013, 1(3): 145 – 149.

[25] MURPHY TL, MURPHY KM. Dendritic cells in cancer immunology [J]. Cellular & Molecular Immunology, 2022, 19(1): 3 – 13.

[26] HERAS-MURILLO I, ADAN-BARRIENTOS I, GALÁN M, *et al*. Dendritic cells as orchestrators of anticancer immunity and immunotherapy [J]. Nature Reviews Clinical Oncology, 2024, 21(4): 257 – 277.

[27] MEHRANI Y, MOROVATI S, KEIVAN F, *et al*. Dendritic cell-based cancer vaccines: The impact of modulating innate lymphoid cells on anti-tumor efficacy[J]. Cells, 2025, 14(11): 812.

[28] WEICHHART T, SÄEMANN MD. The PI3K/Akt/mTOR pathway in innate immune cells: Emerging therapeutic applications[J]. Annals of the Rheumatic Diseases, 2008, 67: iii70 – iii74.

[29] ZHANG L, WU J, LING MT, *et al*. The role of the PI3K/Akt/mTOR signalling pathway in human cancers induced by infection with human papillomaviruses[J]. Molecular Cancer, 2015, 14(1): 87.

[30] POMPURA SL, DOMINGUEZ-VILLAR M. The PI3K/AKT signaling pathway in regulatory T-cell development, stability, and function[J]. Journal of Leukocyte Biology, 2018, 103(6): 1065 – 1076.

[31] CHEN T, LI B, QIU Y, *et al*. Functional mechanism of ginsenosides on tumor growth and metastasis[J]. Saudi Journal of Biological Sciences, 2018, 25(5): 917 – 922.

[32] ALI M, WANI SU, SALAHUDDIN M, *et al*. Recent advance of herbal medicines in cancer-a molecular approach[J]. Heliyon, 2023, 9(2): e13619.

[33] ALJABALI AA, BASHATWAH RM, EL-TANANI M, *et al*. Natural anticancer drugs: Efficacy, safety, and future challenges[J]. Current Medicinal Chemistry, 2025, 32(31): 6764 – 6805.

[34] ALJABALI AA, OBEID MA, BASHATWAH RM, *et al*. Phytochemicals in cancer therapy: A structured review of mechanisms, challenges, and progress in personalized treatment[J]. Chemistry & Biodiversity, 2025, 22(8): e202402479.